Effect of a pre-oxide on the high temperature steam oxidation of Zircaloy-4 andM5 alloys

Matthieu Le Saux, J.C. Brachet, V. Vandenberghe, E. Rouesne, S. Urvoy, A. Ambard, R. Chosson

Effect of a pre-oxide on the high temperature steam oxidation of Zircaloy-4 and M5$_{Framatome}$ alloys

M. Le Saux [a, b*], J.C. Brachet [a], V. Vandenberghe [a, c], E. Rouesne [a], S. Urvoy [a], A. Ambard [d], R. Chosson [e]

[a] *DEN-Service de Recherches Métallurgiques Appliquées (SRMA), CEA, Université Paris-Saclay, F-91191 Gif-sur-Yvette, France*

[b] *Now at ENSTA Bretagne, UMR CNRS 6027, IRDL, F-29200 Brest, France*

[c] *Now at DEN-Service d'Etudes Mécaniques et Thermiques (SEMT), CEA, Université Paris-Saclay, F-91191 Gif-sur-Yvette, France*

[d] *EDF R&D, MMC Department, avenue des Renardières, 77818 Moret-Sur-Loing, France*

[e] *Framatome, 10 rue Juliette Récamier, 69456 Lyon, Cedex 06, France*

Highlights

- Steam oxidation and hydrogen pickup at high temperature are influenced by a pre-oxide.
- The effect of the pre-oxide depends on its thickness and pre-oxidation conditions.
- Pre-oxide is partly reduced before a fresh oxide grows at high temperature.
- Quantity of oxygen diffusing through the metallic substrate at high temperature is nearly the same either there is a pre-oxide or not.

Abstract

The effect of a pre-existing oxide layer formed at low temperature on the subsequent oxidation in steam at high temperature was studied for Zircaloy-4 and M5$_{Framatome}$ alloys. Various pre-oxidation conditions (air at 550°C, steam at 415°C, static and flowing water at ~350°C), pre-oxide thicknesses (3 to 60 µm) and high temperature oxidation conditions (850 to 1200°C, 55 to 9500s) were investigated. Pre-oxide has an effect on the oxidation kinetics and the hydrogen uptake at high temperature, depending on the pre-oxide thickness, the pre-oxidation conditions, the alloy and the high temperature oxidation conditions.

Keywords: Zircaloy-4, M5$_{Framatome}$, oxidation in steam at high temperature, pre-oxide, LOCA

* Corresponding author. Tel.: +33 2 98 34 88 64; fax: +33 2 98 34 87 30.
Email address: matthieu.le_saux@ensta-bretagne.fr (M. Le Saux)

1. Introduction

In some hypothetical accidental scenarios in nuclear Pressurized Water Reactors (PWR), such as LOss of Coolant Accidents (LOCA), fuel cladding tubes made of zirconium alloys can be exposed for a few minutes to steam at High Temperature (HT, up to 1200°C) before being cooled and then quenched in water by the emergency core cooling systems. During in-service operation, an oxide layer appears on the outer surface of the cladding due to corrosion by the water environment (155 bar, ~300-340°C at the cladding surface, with Li, B and H_2). The thickness of this outer pre-oxide layer can reach several tens of microns after several years depending on the alloy and the in-reactor exposure conditions. An oxide layer may also form on the cladding inner surface due to chemical-physical interaction with the fuel.

A review of the data available in the literature has shown that a pre-existing oxide layer may have an influence on the subsequent oxidation of the material under steam at HT. Most of these data are summarized in Table 1 for Zircaloy-4 (Zy-4) and $M5_{Framatome}$[†] alloys, pre-oxidized out-of-pile or in PWR. The results show that the oxidation in steam at HT is delayed in the presence of a pre-existing oxide layer. The effect of the pre-oxide seems to depend on the alloy and the conditions of both pre-oxidation and oxidation at HT. In most cases, the thicker the pre-oxide, the larger the delay in the oxidation at HT. However, some results show that the protective effect of the pre-oxide in terms of weight gains deteriorates beyond a given pre-oxide thickness, varying from one study to another (10 µm according to [3], between 30 and 80 µm according to [9] or 40 µm according to [10][11]), probably due to the differences in pre-oxidation conditions. Nevertheless, the weight gain at HT of the pre-oxidized material never exceeds (or only slightly) that of the non-pre-oxidized material.

With the exception of a few specific conditions (post-breakaway oxidation at temperatures typically lower than 1050°C [4][15][16][20][21], oxidation under high steam pressures [22][23] or secondary hydriding due to steam starvation inside the cladding after ballooning and burst [24][25]), as-received zirconium alloys do not absorb a significant amount of hydrogen when oxidized in steam at HT [26]. Hydrogen pickup during oxidation in steam at HT is not provided in most papers dealing with the oxidation of pre-oxidized zirconium alloys. The scarce data available (see Table 1) show that the pre-oxidized materials may

[†] $M5_{Framatome}$ is a registered trademark of Framatome or its affiliates, in the USA or other countries.

absorb hydrogen during HT oxidation while the non-pre-oxidized materials oxidized under the same conditions do not.

The mechanical behaviour of the cladding during and after cooling from HT can be modified by oxidation and hydrogen [15][20][27][28][29][30]. Thus, the effect of a pre-existing oxide layer on the oxidation kinetics and the hydrogen pickup of the cladding material during subsequent exposure under steam at HT is an important issue.

This work aims at improving both experimental databases and knowledge on the effect of a pre-existing oxide layer on the oxidation of Zr alloys under steam at HT. The influences of the alloy, the pre-oxidation condition, the pre-oxide thickness and the condition of oxidation at HT are investigated. The materials and the experimental procedures used for this study are described in Section 2. The results are presented in Section 3 and further discussed in Section 4. Part of the results has already been reported elsewhere [27][31].

2. Materials and experimental procedures

2.1. Materials and conditions of pre-oxidation

The experiments were made on stress-relieved annealed low tin Zy-4 and fully recrystallized $M5_{Framatome}$ cladding tube samples, with an outer diameter and a thickness of 9.5 and 0.57 mm, respectively. The nominal chemical compositions of the materials are given in weight % (wt%) in Table 2. Samples (2 to 7.5 mm-long) were pre-oxidized up to 2160 days in various conditions: ambient air at 550°C, steam at 415°C, static water at 340-360°C with a typical PWR primary water chemistry, flowing water at 350°C with typical PWR primary water thermal-hydraulic and chemical environment. The purpose of this parametric study was to investigate the sensitivity to pre-oxidation conditions and thus to pre-oxide microstructure, in order to improve the understanding of the effect of a pre-oxide layer on HT oxidation and eventually to provide insights for assessing the effect of a pre-oxide formed in reactor. Pre-oxide thicknesses were deduced from the measured weigh gain values by considering that one micron of zirconia corresponded to a surface weight gain per unit surface area of 0.15 mg/cm^2. Pre-oxide thicknesses ranged from 3 to 60 µm. The samples absorbed more or less hydrogen during pre-oxidation depending on the conditions. Hydrogen contents at the end of pre-oxidation were either measured by using an inert gas fusion thermal conductivity (hot extraction) technique (on the samples then oxidized at HT or on equivalent samples, including the oxide layers) or estimated from known correlations between weight gain and hydrogen

pickup established from data obtained on other Zy-4 and $M5_{Framatome}$ samples pre-oxidized in the same conditions. Pre-oxidation conditions and hydrogen contents of the tested samples are given in Table 3 for Zy-4 and Table 4 for $M5_{Framatome}$. Hydrogen contents are related to the total mass of the samples. The slight hydrogen pickup measured for samples pre-oxidized in air at 550°C may be due to humidity in air.

Optical microscopy observations of cross-sections (perpendicular to the tube sample axis) of a selected number of samples confirmed that the pre-oxide layers were homogeneous, similar on the inner and outer surfaces (with the exception of the samples pre-oxidized in flowing water in the Reggae loop, as anticipated) and their thicknesses were consistent with those expected. These observations also showed that the metal/pre-oxide interface was scalloped (undulations with microscale amplitude and wavelength). The microstructure of the pre-oxide layers depended on their thickness and the conditions under which they were formed. The pre-oxide layers of a few microns thick appeared dense (*i.e.* low porosity) and adherent to the metal on optical micrographs. Networks of cracks parallel to the pre-oxide surface (called circumferential cracks) were observed within thicker pre-oxides (Fig. 1). In pre-oxide layers of several tens of microns thick (> 30 µm typically), cracks perpendicular to the pre-oxide surface (called radial cracks) were evidenced in the outer part of the layer (they did not seem to reach the metal/oxide interface). These circumferential and radial cracks were more numerous and open in pre-oxides formed in air at 550°C than in layers formed in water at 340-360°C (Fig. 1).

2.2. Oxidation in steam at high temperature

Oxidation tests were performed in pure steam (no carrier gas) at atmospheric pressure at 850, 900, 1000 and 1200°C, with holding times between 55 and 9500s depending on the oxidation temperature. The conditions of oxidation in steam at HT tested for each pre-oxidation condition are given in Table 3 for Zy-4 and Table 4 for $M5_{Framatome}$. Some of the samples were oxidized on both their outer and inner surfaces (two-side oxidation); in that case, 20 to 40 mm-long samples were used. Other samples, 32 to 40 mm-long, were oxidized on their outer surface only (one-side oxidation). To prevent steam from coming into contact with the cladding inner surface, non-pre-oxidized end caps in Zircaloy-4 were welded under secondary vacuum at both extremities. The oxidation of end-caps was included in the weight gain measurements (the surface of end caps represented approximately 35% of the total surface of the specimen exposed to steam). In the tested conditions, end-caps are expected to oxidize at a

faster rate than the cladding sample. As a consequence, the weight gains reported for the one-sided oxidized specimens probably overestimate the actual weight gain of the cladding samples, in particular for the longest oxidation times. The oxidation behaviour was probably affected in the immediate vicinity of the welds but no detrimental effect was expected on the overall oxidation of the sample. Post-oxidation observations have shown that oxidation was uniform along the cladding sample (maximal variation of the oxide thickness of a few percent typically), including near the end-caps. It cannot be excluded that hydrogen pickup was promoted in the vicinity of the welds. However, it is supposed that the hydrogen potentially absorbed at sample ends during oxidation at HT did not have time to diffuse very far, excepting eventually for the longest oxidation times tested. Thus, the results of one-side oxidation tests are potentially less accurate for the longest oxidation times tested, nonetheless without questioning the main conclusions.

Oxidation at HT was carried out by using two facilities respectively called DEZIROX 1 and CINOG HP [20][21][23][27]. Both one-side and two-side oxidations were performed in DEZIROX 1. Only two-side oxidation tests were carried out in CINOG HP. For one-side oxidation, the sample hanged from an alumina holder via a hole in the sample upper end-cap. For two-side oxidation, the bottom end of the sample was positioned on an alumina holder allowing free access of steam to both inner and outer surfaces of the sample. Steam was produced from an electrode-type steam generator in DEZIROX 1 and from demineralized water in CINOG HP. Steam flow was directed down through an alumina chamber in DEZIROX 1 and a quartz-tube chamber in CINOG HP. The steam flow rate normalized to the cross-sectional area of the steam chamber was about 70 mg/(cm^2·s) in DEZIROX 1 and 140 mg/(cm^2·s) in CINOG HP, which was sufficient to avoid steam starvation [32][33]. The samples were heated to the desired temperatures by using a vertical resistive furnace in DEZIROX 1 and an induction coil in CINOG HP.

In DEZIROX 1, the samples were inserted into the furnace once it was tuned and stabilized at the target isothermal temperature and flushed with steam for at least 1 hour. The power to the furnace was controlled via a built-in thermocouple. The set-point temperature was fixed before testing using a rod equipped with type S (PtRh-Pt) thermocouples, inserted at the same position as the sample into the furnace. Furthermore, temperature benchmarks are regularly performed on specimens equipped with type S thermocouples spot-welded on their outer surface. The samples reached the target temperature approximately 30s after their introduction into the furnace, for all temperatures tested. The oxidation time commenced when the sample

was placed into the furnace. After isothermal holding, the samples were directly quenched in water down to room temperature.

In the CINOG HP facility, the specimens were heated at 20°C/s up to the set-point oxidation temperature without any temperature overshoot. The outer temperature of the samples was measured in the region near their mid-length using two optical pyrometers. One pyrometer was used to monitor the temperature (feedback to the furnace power) and the other one was used to check the temperature. The oxidation time commenced when the oxidation temperature was reached. After the HT oxidation, the specimens were cooled down by shutting off the induction heating. The achieved cooling was quite fast (cooling rate between 100 and 150°C/s down to 500°C) but significantly slower than during a direct water quench. The absence of temperature overshoot was verified for both facilities. Temperature variation around the target temperature was lower than ±5°C. Temperature gradient was lower than 10°C along the samples oxidized in DEZIROX 1 and along the 5 mm-long central region of the samples oxidized in CINOG HP.

As partly shown in [23], it was checked beforehand, by performing comparative tests on non-pre-oxidized materials, that the results obtained in the two facilities are comparable.

Sample dimensions and weight were measured before and after testing with an accuracy of 10^{-3} mm for diameter and thickness, 10^{-2} mm for length and 0.1 mg for weight.

2.3. Characterizations after oxidation at high temperature

Hydrogen content measurements were performed by an inert gas fusion thermal conductivity technique (HORIBA EMGA-821 and LECO RH404 analysers) on samples extracted from a select number of samples oxidized at HT. Two to four hydrogen content measurements were performed per sample, on pieces generally cut from the middle part of the sample. The oxide layers were not removed before hydrogen analysis so that the reported hydrogen contents are related to the total mass of the samples. The hydrogen content absorbed during oxidation at HT, C_{Ha}, was deduced from the difference between average hydrogen contents measured after and before oxidation, in weight ppm (wppm). The hydrogen content of the samples two-side oxidized was divided by a factor two approximately (ratio between the cladding outer diameter and the sum of its inner and outer diameters) to be compared to the hydrogen content of one-sided oxidized samples, assuming that hydrogen absorption is the same through the outer surface and the inner surface. Indeed, the outer and inner oxide layers showed rather similar aspect and thickness. In a few cases, negative hydrogen pickup values were obtained.

They did not reveal desorption of hydrogen during the treatment at HT *a priori*; they were rather due to the uncertainties on the hydrogen contents before oxidation at HT: these contents were sometimes estimated from measurements performed on other dedicated samples, and besides it is possible that hydrogen was not uniformly distributed within some of the samples.

The hydrogen pickup fraction, f_{Ha}, has been defined as the ratio of the hydrogen absorbed by the material over the total hydrogen generated during the oxidation. It was calculated as follows:

$$f_{Ha} = \frac{M_O}{2M_H} \frac{10^{-6} C_{Ha} m_t}{(1-10^{-6} C_{Ha}) m_t - m_{t0}} \quad (1)$$

where M_O and M_H are the atomic masses of oxygen and hydrogen respectively, m_t is the total mass of the oxidized sample and m_{t0} is its mass before oxidation. This is a mean (integrated) value of the fraction of hydrogen absorbed from the beginning of oxidation, not an "instantaneous" value.

Several layers can be observed after cooling in the samples pre-oxidized then oxidized at HT: a ZrO_2 oxide layer (remaining pre-oxide and/or oxide formed at HT), a metallic layer of oxygen-stabilized α_{Zr} phase (hexagonal close-packed structure) called $\alpha_{Zr}(O)$ containing 2 to 7 wt% of oxygen, and a prior-β_{Zr} layer (with a typical Widmanstätten or parallel-lath structure morphology resulting from the transformation of the β_{Zr} phase, with a body-centered cubic structure, into the α_{Zr} phase, during quenching) or a two-phase α_{Zr} + prior-β_{Zr} layer depending on the oxidation temperature. The microstructure and the thickness of the different layers were observed by microscopy on polished transverse cross-sections obtained from the middle part of selected samples that had been oxidized at HT (Fig. 2). One should keep in mind that the observations were made after cooling down to room temperature. They were not necessarily representative of the state of the oxide at HT, before cooling: the oxide can be damaged during cooling, under the effect of internal stresses generated from phase transformations of the metal and the oxide, and from differences between the thermal coefficients of the different phases/layers constituting the oxidized cladding material [34].

Optical microscopy was used to measure the oxide thickness (measurement uncertainty of a few microns). When the thickness of the oxide layer was expected to be low, a nickel coating was applied before imbedding and polishing the sample on its inner and outer surfaces in order to stabilize the oxide layer and minimize the end effects during polishing. As already

done in [23] and [27], Scanning Electron Microscopy (SEM) (mainly in back scattered electron mode) and a specific image analysis procedure were used to measure the fractions of $\alpha_{Zr}(O)$ and prior-β_{Zr} across the cladding wall thickness. In the following, the so-called $\alpha_{Zr}(O)$ phase layer corresponds to the "continuous" $\alpha_{Zr}(O)$ phase layer containing more than 90% of $\alpha_{Zr}(O)$. The measurements of oxide and $\alpha_{Zr}(O)$ phase thicknesses were performed at two to four azimuthal locations per sample.

The oxygen concentration profile across the wall thickness of a selected number of samples was quantified by Electron-Probe Micro Analysis (EPMA) (CAMECA SX100 electron microprobe) with a typical accuracy of ±0.1 wt%. The measured data were corrected from surface contamination.

3. Results

3.1. Results obtained in the same conditions on the non-pre-oxidized materials have already been partly presented in previous papers [20][21][23][25][27][31]. The facility used and the type of oxidation applied (one-side or two-side) are specified in Table 3 for Zy-4 and Table 4 for M5$_{Framatome}$. The oxidation conditions applied on the pre-oxidized materials were similarly applied on the non-pre-oxidized materials. Oxidation at 850°C

After 600s at 850°C, the samples with 3-8 µm-thick pre-oxides formed in static water at 360°C or 5 µm-thick pre-oxides formed in air at 550°C have lower weight gains than the non-pre-oxidized materials (Fig. 3). The thicker the pre-oxide layer the lower the weight gain. In the case of Zy-4, the weight gains of samples with 5 µm-thick pre-oxides formed in air at 550°C were higher than those expected for the same pre-oxide thickness formed in water at 360°C, and a significant hydrogen pickup was observed (about 100 wppm, $f_{Ha} \approx 30\%$) while it was negligible or very low for the as-received material or the material with 8 µm-thick pre-oxides formed in water at 360°C. In the case of M5$_{Framatome}$, weight gains were close, whether the pre-oxide have been formed under air at 550°C or under water at 360°C, and no hydrogen was measured.

3.2. Oxidation at 900°C

Fig. 4 shows the results obtained after 6000s at 900°C together with those reported in [10][11]. It must be recalled that for this study hydrogen analyses were performed on samples including the oxide layers while the oxide layers had been sandblasted in [10][11]. After

oxidation at HT and quenching, hydrogen is expected to be mainly located in the prior-β_{Zr} layer; $\alpha_{Zr}(O)$ and oxide layers contain only a small amount of hydrogen [25]. Thus, the hydrogen contents measured by keeping the oxide layers may slightly underestimate the hydrogen content within the metal. The weight gain decreases with increasing the pre-oxide thickness, up to about 40 µm (Fig. 4). The weight gains obtained for 4-28 µm-thick pre-oxide layers formed under water at 340-360°C and under O_2 at 425°C were close to one another. However, the material with 7 µm-thick pre-oxides formed under O_2 at 425°C showed a slightly higher weight gain than the one with 8 µm-thick pre-oxides formed under water at 360°C.

While no significant hydrogen pickup was measured for as-received Zy-4 after 6000s at 900°C, the pre-oxidized material absorbed hydrogen, more or less depending on the pre-oxide thickness and the conditions in which it was formed (Fig. 4). According to Guilbert *et al.*' results [11], the hydrogen pickup reduced to the outer surface (*i.e.* hydrogen pickup oxidation divided by approximately a factor two in the case of two-side oxidation) was about 230 wppm for the material with 7 µm-thick pre-oxides formed under O_2 at 425°C, then it decreased with increasing the pre-oxide thickness, up to about 40 µm. However, the hydrogen pickup fraction remained almost the same (17-18%). This suggests that the decrease in hydrogen pickup as a function of the pre-oxide thickness was related to the delay in the oxidation kinetics caused by the presence of a pre-oxide layer. The hydrogen pickup was larger when the pre-oxidation was carried out under O_2 at 500°C [10] due to a faster oxidation rate, as f_{Ha} has almost the same value.

The amount of hydrogen absorbed at 900°C was three times lower for samples with 8 µm-thick pre-oxides formed under water at 360°C than for samples with 7 µm-thick pre-oxides formed under O_2 at 425°C. Very low or negligible hydrogen pickup was observed after 6000s at 900°C in the case of Zy-4 with 18 and 28 µm-thick pre-oxides formed water at 350-360°C. The results reported in [10] and [11] showed that the weight gains increase with increasing the pre-oxide layer thickness beyond 40 µm when it was formed under O_2 at 425 or 500°C, and the material absorbed a large amount of hydrogen (for example, $f_{Ha} \approx 70\%$ for 64 µm-thick pre-oxides formed under O_2 at 425°C).

3.3. Oxidation at 1000°C

After oxidation shorter than about 5000s at 1000°C, weight gains at a given oxidation time were lower for samples pre-oxidized under water at 340-360°C than for the non-pre-oxidized samples, as shown in Fig. 5 for Zy-4 and Fig. 6 for $M5_{Framatome}$. The thicker the pre-oxide (up to 59 µm for Zy-4 and to 10 µm for $M5_{Framatome}$) the larger the benefit. The benefit was larger for Zy-4 than for $M5_{Framatome}$, for pre-oxide thicknesses from 3 to 10 µm formed under water at 340-360°C: weight gains obtained at a given oxidation time were similar for the two alloys when pre-oxidized while Zy-4 oxidized faster than $M5_{Framatome}$ in the absence of a pre-oxide.

Like for the non-pre-oxidized materials, no significant hydrogen uptake was observed for the materials pre-oxidized in water at 340-360°C oxidized during less than 5000s at 1000°C, with the exception maybe of Zy-4 with 8 µm-thick pre-oxides which has absorbed a few tens of wppm of hydrogen after 1800s, corresponding to 8% of the total hydrogen generated by the oxidation reaction (Fig. 5). A larger hydrogen pickup (~200 wppm when reduced to the outer surface, $f_{Ha} \approx 14\%$) was reported in [11] after 1800s at 1000°C for Zy-4 with 7 µm-thick pre-oxide layers formed in O_2 at 425°C. No significant hydrogen pickup was evidenced after 400 or 1800s at 1000°C for $M5_{Framatome}$ with 3-5 µm-thick pre-oxides formed under water at 360°C (Fig. 6). Guilbert *et al.* [11] observed for Zy-4 pre-oxidized in O_2 at 425°C an increase of weight gains and hydrogen uptakes after 900 or 1800s at 1000°C when increasing the pre-oxide thickness beyond 40 µm (f_{Ha} reached nearly 100% in the case of 6 µm-thick pre-oxides). However, the results presented herein did not show any significant hydrogen pickup after 400 or 1800s at 1000°C for Zy-4 with 59 µm-thick pre-oxide layers formed under water at 360°C.

After 200s at 1000°C, the weight gain was largely lower for Zy-4 with 50 µm-thick pre-oxides formed in air at 550°C than for the non-pre-oxidized material, but the first one has absorbed hydrogen (about 70 wppm, $f_{Ha} \approx 44\%$) while the second one has not. After 400s at 1000°C, the presence on Zy-4 of a pre-oxide layer of 5, 25 or 50 µm formed under air at 550°C induced a decrease in weight gain comparable to that measured for pre-oxides formed under water at 340-360°C, but this was associated with a significant hydrogen pickup (> 100 wppm, corresponding to f_{Ha} values of 18% for 5 µm-thick pre-oxides and 42-43% for 25 and 50 µm-thick pre-oxides).

After 1800s at 1000°C, for both Zy-4 and $M5_{Framatome}$, weight gains of the materials pre-oxidized under air at 550°C were slightly lower in the presence of a 25 µm-thick pre-oxide layer than without pre-oxide, but they were close from each other for 5 and 50 µm-thick pre-oxides, while weight gains were significantly lower when pre-oxides were formed under water at 340-360°C or O_2 at 425°C. In the case of the materials pre-oxidized in air at 550°C, a hydrogen pickup of several hundreds of wppm was measured for Zy-4 after 1800s at 1000°C (Fig. 5), while the hydrogen pickup was significantly lower for $M5_{Framatome}$ (about 90 wppm *i.e.* $f_{Ha} \approx 5\%$ for 50 µm-thick pre-oxides; Fig. 6). The hydrogen content absorbed by Zy-4 pre-oxidized under air at 550°C increased in the course of oxidation. Hydrogen pickup fractions after 1800s at 1000°C were approximately 7, 27 and 17% for pre-oxide thicknesses of 5, 25 and 50 µm, respectively. They were nearly two times lower than after 200 or 400s at this temperature.

The lower weight gains measured in some cases when the material was pre-oxidized was due to a delayed growth of the new oxide layer at HT in the presence of a pre-existing oxide layer. For example, in the presence of a 10 µm-thick pre-oxide, the fresh oxide has not yet begun to grow after 400s at 1000°C. It was observed that the new oxide layer did not grow uniformly at HT, in particular during the growth of the first microns: the metal/oxide interface appeared scalloped.

In the case of Zy-4 with 59 µm-thick pre-oxides formed in water at 360°C, circumferential cracks were observed within the pre-oxide remaining after oxidation during 400s at 1000°C then cooling, as well as a few radial cracks through the oxide layer. After 1800s at 1000°C, a network of circumferential cracks more or less interconnected was evidenced at the interface between the remaining pre-oxide and the oxide formed at HT, as well as radial cracks through the entire thickness of the pre-oxide and through at least a part of the oxide formed at HT (Fig. 7). In some cases, the oxide formed at HT was thicker beneath these radial cracks.

In the case of samples with 50 µm-thick pre-oxides formed under air at 550°C, circumferential cracks together with a few radial cracks were also observed within the pre-oxide remaining after 200 or 400s at 1000°C. After 1800s at this temperature, connected circumferential cracks appeared at the interface between the remaining pre-oxide and the oxide formed at HT, in addition to radial cracks crossing the whole pre-oxide thickness (Fig. 7). The oxide formed at HT also seemed to be damaged.

In the case of samples with 10-13 µm-thick pre-oxides formed in water at 340-350°C, oxidized at 1000°C on their outer surface only, the inner pre-oxide, exposed to vacuum, has progressively reduced during the holding at HT, until it has completely disappeared after a holding time between 420 and 1290s. The thickness of the outer pre-oxide, exposed to steam, only slightly evolved at 1000°C.

After about 5000s at 1000°C, the oxidation kinetics (transition from a sub-parabolic to a nearly linear oxidation kinetics) sped up and the materials absorbed hydrogen (Fig. 5 and Fig. 6); this transition is commonly called breakaway oxidation. For oxidation times longer than 5000s, the weight gain and hydrogen uptake of samples with 10-13 µm-thick pre-oxides formed under water at 340-360°C were close of those of the samples without pre-oxides. The excess in weight gain measured for pre-oxidized $M5_{Framatome}$ samples was essentially due to the faster oxidation of the end-caps in Zircaloy-4 (non-pre-oxidized), included in the weight gain measurements. Thus it can be concluded that the breakaway oxidation resistance of Zy-4 and $M5_{Framatome}$ under steam at 1000°C was not significantly modified by 10-13 µm-thick pre-oxides formed under water at 340-360°C.

3.4. Oxidation at 1200°C

The weight gains after oxidation under steam at 1200°C tended to be lower for the pre-oxidized materials than for the as-received materials, for a given oxidation time (Fig. 8 for Zy-4 and Fig. 9 for $M5_{Framatome}$). The benefit increased with increasing the pre-oxide thickness.

The oxidation at 1200°C was thus delayed in the presence of a pre-existing oxide layer formed at lower temperature. However, the weight gain of the pre-oxidized material progressively caught up with that of the non-pre-oxidized materials in the course of oxidation. After 55-60s at 1200°C, the evolution of weight gains as a function of the pre-oxide thickness followed the same tendency for the materials with pre-oxides of 25 to 36 µm for Zy-4 (Fig. 8) and 13 to 35 µm for $M5_{Framatome}$ (Fig. 9) formed under static water at 360°C, pre-oxides of 15 µm formed under flowing water at 350°C, and pre-oxides of 60 µm for Zy-4 and 30 µm for $M5_{Framatome}$ formed under steam at 415°C.

After 600s at 1200°C, the weight gain progressively decreased with increasing the pre-oxide thickness, in similar ways for Zy-4 samples with 8 to 59 µm-thick pre-oxide layers formed

under water at 360°C tested herein, samples with 9 to 64 µm-thick pre-oxides formed in O_2 at 425°C tested by Guilbert *et al.* [11], and samples with 9 to 33 µm-thick pre-oxides formed in PWR tested by Ozawa *et al.* [1]. However, the samples with 25 and 50 µm-thick pre-oxides formed in air at 550°C or with 30 and 80 µm-thick pre-oxides formed in air at 500°C after pre-hydriding at 400°C [9] had weight gains close to those of the non-pre-oxidized material after 600s at 1200°C.

As-received Zy-4 did not absorb hydrogen when steam oxidized during 600s at 1200°C. On the one hand, for this oxidation condition, the material with pre-oxides of 8 µm formed under water at 360°C, of 25 and 50 µm formed in air at 550°C, or thinner than 40 µm formed under O_2 at 425°C [11] did not absorb a significant amount of hydrogen. On the other hand, an important hydrogen pickup was reported in [11] for pre-oxides thicker than 40 µm formed in O_2 at 425°C. This hydrogen pickup increased with increasing the pre-oxide thickness, due to an increase of the hydrogen pickup fraction (about 16% for 64 µm-thick pre-oxides). The material with 59 µm-thick pre-oxide layers formed under water at 360°C also absorbed some hydrogen when oxidized 600s at 1200°C but in a smaller quantity (about 90 wppm, $f_{Ha} \approx 3\%$).

In some cases, radial cracks, present after pre-oxidation or formed at the beginning of the holding at HT, were observed in the pre-oxide layers. The new oxide started to form in the vicinity of these radial cracks at HT then tended to grow uniformly. The same observations were reported for samples corroded in PWR [36]. The interface between the prior-β_{Zr} and the α_{Zr}(O) layers, *i.e.* the diffusion depth of oxygen through the metallic substrate, was not significantly affected nonetheless by the sooner oxidation around the cracks in the pre-oxide. Indeed, the diffusion of oxygen far from the metal/oxide interface is driven by the diffusion in volume of oxygen into the α_{Zr}(O) layer. Thus, the heterogeneous oxidation at the beginning of oxidation at HT did not seem to alter the later oxidation.

As illustrated in Fig. 8, and as previously shown for oxidation at 1000°C, the lower weight gains measured at 1200°C in the presence of a pre-oxide were due to a delayed oxide growth at HT. Nevertheless, the overall quantity of oxygen that diffused into the metallic substrate was the nearly same whether there was a pre-oxide layer or not. Indeed, the oxygen coming from the reduction of the pre-existing oxide at the ZrO_2/α_{Zr}(O) interface has diffused into the metallic part, causing thickening of the α_{Zr}(O) phase layer (Fig. 10 (a)) and associated oxygen

diffusion into the β_{Zr} layer. Fig. 11 compares oxygen concentration profiles measured by EPMA, after oxidation during approximately 60s at 1200°C, within the prior-β_{Zr} layer of samples with 13-15 µm or 36 µm-thick pre-oxide layers and of non-pre-oxidized samples, as-received and pre-hydrided. For this oxidation condition, no fresh oxide has grown yet at HT in the sample with 36 µm-thick pre-oxides and only a few microns of fresh oxide have formed in the sample with 13-15 µm-thick pre-oxide layers. It was shown that the oxygen concentration profile within the prior-β_{Zr} layer was nearly the same for the pre-oxidized materials and the non-pre-oxidized materials containing a similar hydrogen content. The oxygen content is slightly larger than in the as-received material oxidized in the same conditions due to the effect of hydrogen on the solubility of oxygen in β_{Zr}, already reported in [25][27][31][39].

The results illustrated in Fig. 10 (b) showed that the pre-oxide reduced at the beginning of oxidation whether the surface was exposed to vacuum or to steam. On the one hand, the pre-oxide whose surface was exposed to steam reduced from only a few microns. Its thickness then did not evolve anymore because the inward flux of oxygen in the oxide became higher than the inward flux in the α_{Zr}(O) phase [35], leading the growth of a new oxide layer beneath the remaining pre-oxide. On the other hand, reduction of the inner pre-oxide in contact with vacuum continued until it had completely disappeared. For example, complete reduction was achieved after a holding time between 187 and 520s at 1200°C for 24-26 µm-thick pre-oxides, and between 60 and 202s for 13-15 µm-thick pre-oxides. As long as the pre-oxide was not fully reduced, the growth kinetics of the α_{Zr}(O) phase layers were similar at the outer and inner peripheries of the samples one-sided oxidized at 1200°C: the α_{Zr}(O) phase layer grows at the same rate whether it is associated with the reduction of the pre-existing oxide or the growth of a fresh oxide at HT (Fig. 10). When the pre-oxide was completely reduced on the side non-exposed to steam, the thickness of the α_{Zr}(O) phase deriving from this reduction kept increasing in the case of Zy-4 with 24-26 µm-thick pre-oxides formed under water at 360°C until at least 1492s at 1200C°C. In the case of $M5_{Framatome}$ with 13-15 µm-thick pre-oxides formed under water at 360°C, the thickness of the inner "continuous" α_{Zr}(O) phase layer, not exposed to steam, slightly decreased during the holding at 1200°C. Indeed, when this relatively thin pre-oxide layer was entirely reduced, *i.e.* when there was no oxygen source anymore, the α_{Zr}(O) phase was progressively depleted in oxygen and transformed into the β_{Zr} phase, as predicted by diffusion calculations [33].

As illustrated in Fig. 10, the results obtained on Zy-4 and $M5_{Framatome}$ with 24-26 µm-thick and 13-15 µm-thick pre-oxides respectively, showed that when a new oxide layer began to grow at HT beneath the outer pre-oxide, exposed to steam, the $\alpha_{Zr}(O)$ phase layer grew faster than in the case of the non-pre-oxidized material. This may be due to a faster diffusion of oxygen through the $\alpha_{Zr}(O)$ phase when formed during the growth of this new oxide layer, which may be due for example to a particular stress state at the metal/oxide interface, to hydrogen pickup or to more heterogeneous thickness of the $\alpha_{Zr}(O)$ phase. Further investigation is needed to understand these effects.

4. Discussion

4.1. Oxidation and oxygen diffusion

The results have shown that the oxidation under steam at HT is delayed in most cases in the presence of a pre-oxide. The oxidation kinetics of the pre-oxidized material then catches up that of the non-pre-oxidized material: the fresh oxide tends to grow more quickly at HT depending on the pre-oxidation conditions.

The oxidation process under steam at HT of materials with pre-existing oxides involves two main steps, both associated with diffusion of oxygen through the metallic substrate: the pre-oxide layer first reduces at the beginning of the treatment at HT, then a new oxide grows at the metal/oxide interface (Fig. 12). This can be explained by the oxygen flux balance at the metal/oxide interface [35]: at the beginning of the holding at HT, the inward flux of oxygen in the pre-oxide J_O^{ox} is lower than the inward flux in the $\alpha_{Zr}(O)$ phase J_O^{α}; later, the balance of the fluxes at the metal/oxide interface reverses, due to the decrease of the oxygen flux in the $\alpha_{Zr}(O)$ phase layer and the increase of the flux in the oxide layer, resulting from their respective thickening and thinning.

The pre-oxide and the oxide formed at HT have quite different (micro)structures. For example, the grains of the oxides formed at HT tend to be wider and more columnar than those formed at lower temperature and, with the exception of post-breakaway oxidation conditions, the oxides formed at HT usually do not show circumferential cracks. This may have an effect on the transport properties, of oxygen in particular. According to Mazères *et al.* [35], the effective coefficient of diffusion of oxygen at HT may be lower within the pre-oxide during its reduction than within the oxide formed at HT. The relatively fast growth kinetics of the new oxide at HT is still not clearly explained. As suggested in [35], the pre-oxide may be

damaged and may lose, at least partially, its protective effect regarding oxygen diffusion when a fresh oxide layer starts to grow at HT. This may be associated with change in stoichiometry and phase transformation of zirconia, inducing volume changes and resulting in crack formation. It is also possible that oxygen diffusion in the $\alpha_{Zr}(O)$ phase is slower when this phase results from the reduction of the pre-oxide than when it forms during the growth of the new oxide layer at HT. Furthermore, diffusion of oxygen may be faster through the oxide formed at HT (beneath the remaining pre-oxide and the $\alpha_{Zr}(O)$ phase resulting from the partial reduction of the pre-oxide) than through the oxide formed at HT directly from the as-received metal, due to different microstructure (morphology of crystallites, …), porosity or stress state for example.

At HT, hydrogen mainly concentrates into the β_{Zr} phase layer [25][27][37][38]. The solubility limit of oxygen in the β_{Zr} phase is increased in the presence of hydrogen [25][27][39]. After oxidation at HT, an enrichment in hydrogen is generally observed at the interface between the $\alpha_{Zr}(O)$ layer and the prior-β_{Zr} layer [37][38]. This enrichment may have an effect on the solubility limit of oxygen at this interface. Moreover, the diffusion of oxygen may be accelerated in the presence of hydrogen [27][35]. Therefore it cannot be excluded that the hydrogen absorbed during pre-oxidation (when it was carried out under water or steam in particular) or during oxidation at HT, has an influence on the actual oxidation and hydrogen pickup at HT. However, no significant effect on these processes of a pre-hydriding up to 600 wppm was observed in [20].

Although the growth of a fresh oxide at HT is in some cases delayed in the presence of a pre-oxide, the overall quantity of oxygen that diffused into the metallic substrate was nearly the same whether there was a pre-oxide layer or not. Indeed, the pre-oxide is a source of oxygen, as efficient as the outer steam. The mechanical behaviour of the material oxidized at HT is directly correlated to the amount of oxygen having diffused within the metal (excluding additional effect of hydrogen) [27][40][41]. Thus, as shown by mechanical tests performed at 20 and 135°C [11][31], the residual ductility of pre-oxidized samples oxidised at HT and quenched is close to that of the non-pre-oxidized samples containing the same hydrogen content and oxidized under similar conditions.

4.2. Hydrogen pickup

It was observed that in some conditions the pre-oxidized materials absorb hydrogen during oxidation at HT while the non-pre-oxidized materials do not. This supports the hypothesis that the oxide formed at HT after reduction of a pre-existing oxide does not have the same characteristics than the oxide directly formed from the bare metal.

Similar hydrogen pickup fractions were measured after 200 and 400s at 1000°C for Zy-4 with pre-oxides of 5, 25 and 50 µm formed under air at 550°C. The hydrogen pickup fraction (average value from the beginning of the oxidation) was lower after 1800s at this same temperature. To explain this decrease of the hydrogen pickup fraction, one can assume that the hydrogen pickup fraction has not evolve much until the fresh oxide had not yet begun to grow or remained relatively thin, then decreased (or even became negligible) from a given thickness of oxide formed at HT, and finally increased again when this thickness became important.

The hydrogen pickup fraction depends on the pre-oxidation conditions, the pre-oxide thickness, the alloy and the conditions of oxidation at HT: it varies from 0 up to several tens of percent. During in-service operations in PWR, the cladding material absorbs from 10 to 20% of the hydrogen generated from the corrosion reaction, depending on the alloy and the corrosion conditions [42]. The material can absorb higher hydrogen pickup fractions at HT partly because hydrogen (in solid solution) diffuses faster in the metal and the oxide.

As shown by Guilbert *et al.* [11], the hydrogen pickup of the pre-oxidized materials at HT can have consequences on their residual mechanical behaviour, since hydrogen has an embrittlement effect at low temperature [18][27][28][29][30][41].

4.3. Corrosion and hydrogen pickup mechanisms

The oxidation kinetics and the hydrogen pickup are linked to the characteristics of the oxide, pre-existing or formed at HT: grains morphology, cohesion between grains, density, location of pores (resulting from clustering of vacancies for example) and cracks.

When the fraction of hydrogen absorbed is high (several tens of percent), it may be assumed that dissociation of water and reduction/recombination of hydrogen have mainly occurred at the vicinity of the metal/oxide interface. This presupposes that steam had access to the metal

through a network of open pores and/or interconnected cracks in the oxide (transport in the gas phase). This access is facilitated by the presence of radial cracks within the oxide, as observed for example before and after oxidation at HT in samples with 50 µm-thick pre-oxides formed under air at 550°C (Fig. 1 and Fig. 7). However, these cracks generally do not cross the whole thickness of the oxide layer. Pores and circumferential cracks within the oxide may therefore also contribute to the transport of steam to the metal. This network of interconnected defects may act as a "hydrogen pump" [43][44]: because of the oxidation of the metal, the partial pressure of gaseous hydrogen in pores and cracks near the metal/oxide interface would increase, leading to an additional hydrogen pickup, if it is assumed that the hydrogen absorbed by the metal comes from the dissolution of gaseous hydrogen (so that the solubility of hydrogen in the metal is proportional to the square root of the hydrogen partial pressure, following the Sieverts's law). Due to the resulting pressure decrease within these cracks, steam would be "sucked up" again. In theory, this process could be repeated until the hydrogen content in the metal is in equilibrium with the local hydrogen partial pressure in the atmosphere filling the cracks close to the metal-oxide interface (hydrogen pickup may be much larger than given by equilibrium with the ambient hydrogen concentration).

In cases where hydrogen pickup is lower (a few percent typically), dissociation of water and reduction/recombination of hydrogen may have taken place within the oxide layer, not far from the metal/oxide interface, at the interface between a "porous" oxide sublayer (presence of pores and interconnected cracks, weak intergranular cohesion due to disoriented grain boundaries for example) and a "dense" oxide sublayer. Indeed, a more or less continuous network of cracks or porosity nearly parallel to the metal/oxide interface have been observed in some cases near the interface between the remaining pre-oxide and the oxide formed at HT, or at the metal/oxide interface. Guilbert *et al.* [11] suggested that these interconnected cracks/porosity result from the clustering of the circumferential cracks initially present in the pre-oxide, during reduction of the pre-oxide (the cracks progressively move closer to the interface with the metal). The diffusion of hydrogen through the "dense" oxide sublayer, mainly via vacancies and interstitials *a priori*, would lead to a local enrichment in hydrogen at the metal/oxide interface, high enough for the metal to absorb hydrogen.

When there is no hydrogen pickup at HT, it may be assumed that dissociation of water and reduction/recombination of hydrogen have occurred at the outer surface or within the existing oxide but far from the interface with the metal, so that the potential access of hydrogen to the

metal (by solid state diffusion) would be relatively slow. The amount of hydrogen at the metal/oxide interface would remain too low for the metal to absorb hydrogen.

In the cases of pre-oxides formed under air at 550°C, the fraction of hydrogen absorbed by the material was lower after 600s at 1200°C than after 1800s at 1000°C, and even more than after 6000s at 900°C. As proposed in [11], this reduction of the hydrogen pickup fraction with increasing the oxidation temperature may be attributed to the fact that the solid state diffusion through the oxide is a thermally activated process (whose rate increases exponentially with temperature), while the transport in the gas phase shows a lower temperature dependence. Therefore, it may be assumed that the relative contribution of the gas phase transport, expected to be responsible for high hydrogen pickup fractions, to the transport of oxygen and hydrogen species decreases with increasing the temperature. This may also be related to the influence of temperature on the oxide structure and microstructure [45], which can have an effect on the transport of hydrogen species.

5. Conclusions

The effects of a pre-existing oxide layer on the subsequent oxidation under steam at HT was studied for Zy-4 and $M5_{Framatome}$ alloys. Oxidation tests were performed under steam (at atmospheric pressure) at 850, 900, 1000 and 1200°C, for holding times between 55 and 9500s, on samples with pre-oxides thicknesses between 3 and 60 µm, formed under various conditions (air at 550°C, steam at 415°C, static water at 340-360°C with a typical PWR primary water chemistry, flowing water at 350°C with typical PWR primary water thermal-hydraulic and chemical environment).

It was shown that the HT steam oxidation is generally delayed in the presence of a pre-oxide. The thicker the pre-oxide, the more pronounced the effect is. The pre-oxide reduces at the beginning of oxidation at HT then a fresh oxide grows when the oxygen flux balance at the metal/oxide interface reverses. Both processes are associated with diffusion of oxygen through the metallic substrate. The overall quantity of oxygen that diffuses into the metal is nearly the same whether it is associated with reduction of the pre-oxide or growth of a new oxide. The oxidation kinetics of the pre-oxidized material progressively catches up that of the non-pre-oxidized material in the course of oxidation at HT. In the conditions that have been tested, the oxidation kinetics of the pre-oxidized material never exceeds that of the non-pre-oxidized material, with the exception of 50 µm-thick pre-oxides formed under air at 550°C. The difference between the oxidation rates of Zy-4 and $M5_{Framatome}$ at 1000°C are reduced in

the presence of a pre-oxide. The resistance to breakaway oxidation under steam at 1000°C is not significantly modified by pre-oxidation. At given pre-oxide thickness and HT oxidation conditions, the growth rate of the fresh oxide at HT depends on the pre-oxidation conditions. Typically, HT oxidation is often faster after pre-oxidation under air at 550°C than with pre-oxides formed under water at 340-360°C.

In some cases, the pre-oxidized materials absorb hydrogen during oxidation under stream at HT while the non-pre-oxidized materials do not. The hydrogen pickup increases during oxidation, although the fraction of hydrogen absorbed does not. The hydrogen pickup fraction depends on the pre-oxide thickness, the conditions in which it was formed, the alloy, and the conditions of oxidation at HT: it varies from zero to several tens of percent. The pre-oxides may be ranked as follows, from the least to the most protective with respect to hydrogen pickup at HT: air at 550°C, O_2 at 500°C, O_2 at 425°C, water (PWR primary water chemistry) at 340-360°C.

The results suggest that the oxygen and hydrogen transport mechanisms and kinetics, and the locations of water dissociation and hydrogen reduction/recombination at HT may be different whether there was a pre-oxide or not. Further investigations are still needed to improve understanding of the relationship between the characteristics of the pre-oxide, the corrosion mechanisms at HT and their effects on the oxidation and hydrogen pickup at HT, especially for real PWR environment.

6. Acknowledgements

We thank C. Cobac, P. Crébier, D. Gilbon, D. Hamon, C. Hossepied, G. Nony, J. Rousselot and V. Rabeau from CEA, A. Cabrera, M. Blat-Yrieix, P. Jacques and B. Sebbari from EDF, and J.P. Mardon and V. Garat from Framatome, for their contributions to this work.

References

[1] M. Ozawa, T. Takahashi, T. Homma, K. Goto, Behavior of Irradiated Zircaloy-4 Fuel Cladding Under Simulated LOCA Conditions, Zirconium in the Nuclear Industry: Twelfth International Symposium, ASTM STP 1354, G.P. Sabol and G.D. Moan, Eds, American Society for Testing and Materials, West Conshohocken, PA, 2000, pp. 279-299.

[2] T. Chuto, Oxidation of high burnup fuel cladding in LOCA conditions, Fuel Safety Research Meeting 2010, Tokai, Japan, May 19-20, 2010.

[3] S. Leistikow, G. Schanz, H.V. Berg, Kinetics and morphology of isothermal steam oxidation of Zircaloy-4 at 700-1300 C, Report KFK 2587, Kernforschungszentrum Karlsruhe, 1978.

[4] S. Leistikow, G. Schanz, Oxidation Kinetics and Related Phenomena of Zircaloy-4 Fuel Cladding Exposed to High Temperature Steam and Hydrogen-Steam Mixtures under PWR Accident Conditions, Nuclear Engineering and Design 103 (1987) 65-84.
[5] R.R. Biederman, R.D. Sisson Jr., J.K. Jones, W.G. Dobson, A Study of Zircaloy 4 - Steam Oxidation Reaction Kinetics, NP-734 Final Report, Electric Power Research Institute, 1978.
[6] H. Ocken, R.R Biederman, C.R. Hann, R.E. Westerman, Evaluation Models of Zircaloy Oxidation in Light of Recent Experiments, Zirconium in the Nuclear Industry (Fourth Conference), ASTM STP 681, American Society for Testing and Materials, 1979, pp. 514-536.
[7] S. Kawasaki, T. Furuta, M. Suzuki Oxidation of Zircaloy-4 under High Temperature Steam Atmosphere and Its Effect on Ductility of Cladding, Journal of Nuclear Science and Technology 15 (1978) 589-596.
[8] J.S. Yoo, I.S. Kim, Effect of preoxidation on the Zircaloy-4 oxidation behavior in steam-water mixture between 700°C and 850°C, Journal of the Korean Nuclear Society 19 (1987) 122-129.
[9] J.H. Baek, Y.H. Jeong, Steam oxidation of Zr-1.5Nb-0.4Sn-0.2Fe-0.1Cr and Zircaloy-4 at 900-1200°C. Journal of Nuclear Materials 361 (2007) 30-40.
[10] S. Guilbert, C. Duriez, C. Grandjean, Influence of a pre-oxide layer on oxygen diffusion and on postquench mechanical properties of Zircaloy-4 after steam oxidation at 900°C, International Topical Meeting on Light Water Reactor Fuel Performance, Orlando, USA, September 26-29, 2010, pp. 278-288.
[11] S. Guilbert, P. Lacote, G. Montigny, C. Duriez, J. Desquines, C. Grandjean, Effect of pre-oxide on Zircaloy-4 high temperature steam oxidation and post-quench mechanical properties, Zirconium in the Nuclear Industry: 17th Volume, STP1543, B. Comstock and P. Barbéris, Eds., ASTM International, West Conshohocken, PA, 2014.
[12] K. Park, K.P. Kim, T.G. Yoo, K.T. Kim, Pressure effects on high temperature steam oxidation of Zircaloy-4. Metals and Materials International 7 (2001) 367-373.
[13] K. Park, S. Yang, K. Ho, Steam Pressure Effects on Zr-alloy Oxidation at High Temperatures, 2011 Water Reactor Fuel Performance Meeting, Chengdu, China, September 11-14, 2011.
[14] C. Grandjean, G. Hache, G., A State-of-the-Art Review of Past Programmes Devoted to Fuel Behaviour Under Loss-of-Coolant Conditions. Part 3. Cladding Oxidation. Resistance to Quench and Post-Quench Loads, Technical Report SEMCA 2008-093, Institut de Radioprotection et de Sureté Nucléaire, 2008.
[15] M. Billone, Y. Yan, T. Burtseva, R. Daum, Cladding Embrittlement during Postulated Loss-of-Coolant Accidents, NUREG/CR-6967, Argonne National Laboratory, Lemont, IL, 2008.
[16] M. Steinbrück, N. Vér, M. Grosse, Oxidation of advanced zirconium cladding alloys in steam at temperatures in the range of 600-1200 °C, Oxidation of Metals 76 (2011) 215-232.
[17] Y. Yan, R.V. Strain, T.S. Bray, M.C. Billone, High Temperature Oxidation of Irradiated Limerick BWR Cladding, Report ANL/ET/CP-107073, Argonne National Laboratory, Lemont, IL, 2002.
[18] F. Nagase, High burnup fuel behavior under LOCA conditions, Fuel Safety Research Meeting, Tokyo, Japan, March 2-3, 2005.
[19] T. Chuto, F. Nagase, T. Fuketa, High temperature oxidation of Nb-containing Zr alloy cladding in LOCA conditions, Nuclear Engineering and Technology 41 (2009) 163-170.

[20] L. Portier, T. Bredel, J.C. Brachet, V. Maillot, J.P. Mardon, A. Lesbros, Influence of Long Service Exposures on the Thermal-Mechanical Behaviour of Zy-4 and M5M5™ Alloys in LOCA Conditions, Journal of ASTM International 2 (2005) JAI12468.
[21] V. Vandenberghe, J.C. Brachet, M. Le Saux, D. Gilbon, J.P. Mardon, B. Sebbari, Sensitivity to Chemical Composition Variations and Heating/Oxidation Mode of the Breakaway Oxidation in M5 Cladding Steam Oxidized at 1000°C (LOCA Conditions), TopFuel 2012, Manchester, UK, September 2-6, 2012, European Nuclear Society, Brussels, Belgium.
[22] K. Park, K.P. Kim, T.G. Yoo, K.T. Kim, Pressure effects on high temperature steam oxidation of Zircaloy-4, Metals and Materials International 7 (2001) 367-373.
[23] M. Le Saux, V. Vandenberghe, P. Crébier, J.C. Brachet, D. Gilbon, J.P. Mardon, B. Sebbari, Influence of Steam Pressure on the High Temperature Oxidation and Post-Cooling Mechanical Properties of Zircaloy-4 and M5™ Cladding (LOCA Conditions), Zirconium in the Nuclear Industry: 17th Volume, STP1543, B. Comstock and P. Barbéris, Eds., ASTM International, West Conshohocken, PA, 2014, pp. 1002-1053.
[24] J. Stuckert, M. Große, C. Rössger, M. Klimenkov, M. Steinbrück, M. Walter, QUENCH-LOCA program at KIT on secondary hydriding and results of the commissioning bundle test QUENCH-L0, Nuclear Engineering and Design 225 (2013) 185-201.
[25] J.C. Brachet, D. Hamon, M. Le Saux, V. Vandenberghe, C. Tofflon-Masclet, E. Rouesne, S. Urvoy, J.L. Béchade, C. Raepsaet, J.L. Lacour, G. Bayon, F. Ott, Study of secondary hydriding at high temperature in zirconium based nuclear fuel cladding tubes by coupling information from neutron radiography/tomography, electron probe micro analysis, micro elastic recoil detection analysis and laser induced breakdown spectroscopy microprobe, Journal of Nuclear Materials 488 (2017) 267-286.
[26] J.C. Brachet, V. Vandenberghe, Comments to papers of J. H. Kim et al. [1] and M. Große et al. [2] recently published in JNM "On the hydrogen uptake of Zircaloy-4 and M5™ alloys subjected to steam oxidation in the 1100-1250°C temperature range", Journal of Nuclear Materials 395 (2009) 169-172.
[27] J.C. Brachet, V. Vandenberghe-Maillot, L. Portier, D. Gilbon, A. Lesbros, N. Waeckel, J.P. Mardon, Hydrogen Content, Preoxidation, and Cooling Scenario Effects on Post-Quench Microstructure and Mechanical Properties of Zircaloy-4 and M5™ Alloys in LOCA Conditions, Journal of ASTM International 5 (2008).
[28] H.K. Yueh, R.J. Comstock, B. Dunn, M. Le Saux, Y.P. Lin, D. Lutz, D.J. Park, E. Perez-Fero, Y. Yan, Loss of Coolant Accident Testing Round Robin, TopFuel 2013, Charlotte, NC, September 15–19, 2013, American Nuclear Society, La Grange Park, IL, USA.
[29] J. Desquines, D. Drouan, S. Guilbert, P. Lacote, Embrittlement of Pre-Hydrided Zircaloy-4 by Steam Oxidation under Simulated LOCA Transients, Journal of Nuclear Materials 469 (2016) 20-31.
[30] I. Turque, R. Chosson, M. Le Saux, J.C. Brachet, V. Vandenberghe, J. Crépin, A.F. Gourgues-Lorenzon, Mechanical Behavior at High Temperatures of Highly Oxygen- or Hydrogen-Enriched α and Prior-β Phases of Zirconium Alloys, Zirconium in the Nuclear Industry: 18th International Symposium, ASTM STP1597, R. J. Comstock and A. T. Motta, Eds., ASTM International, West Conshohocken, PA, 2018, pp. 240-280.
[31] M. Le Saux, J.C. Brachet, V. Vandenberghe, D. Gilbon, J.P. Mardon, B. Sebbari, Influence of Pre-Transient Oxide on LOCA High Temperature Steam Oxidation and Post-Quench Mechanical Properties of Zircaloy-4 and M5™ cladding, 2011 Water Reactor Fuel Performance Meeting, Chengdu, China, September 11-14, 2011.

[32] S. Kawasaki, T. Furuta, M. Suzuki, Oxidation of Zircaloy-4 under High Temperature Steam Atmosphere and Its Effect on Ductility of Cladding, Journal of Nuclear Science and Technology 15 (1979) 589-596.
[33] S. Leistikow, G. Schanz, Oxidation Kinetics and Related Phenomena of Zircaloy-4 Fuel Cladding Exposed to High Temperature Steam and Hydrogen-Steam Mixtures under PWR Accident Conditions, Nuclear Engineering and Design 103 (1987) 65-84.
[34] M. Le Saux, T. Guilbert, J.C. Brachet, An approach to study oxidation-induced stresses in Zr alloys oxidized at high temperature, Corrosion Science 140 (2018) 79-91.
[35] B. Mazères, C. Desgranges, C. Toffolon-Masclet, D. Monceau, Experimental study and numerical simulation of high temperature (1100–1250 °C) oxidation of prior-oxidized zirconium alloy, Corrosion Science 103 (2016) 10-19.
[36] F. Nagase, T. Chuto, T. Fuketa, Behavior of High Burn-up Fuel Cladding under LOCA Conditions, Journal of Nuclear Science and Technology 46 (2009) 763-769.
[37] C. Raepsaet, P. Bossis, D. Hamon, J.L. Béchade, J.C. Brachet, Quantification and local distribution of hydrogen within Zircaloy-4 PWR nuclear fuel cladding tubes at the nuclear microprobe of the Pierre Süe Laboratory from μ-ERDA, Nuclear Instruments and Methods in Physics Research B 266 (2008) 2424-2428.
[38] E. Torres, J. Desquines, S. Guilbert, M.C. Baietto, M. Coret, P. Berger, M. Blat, A. Ambard, Hydrogen motion in Zircaloy-4 cladding during a LOCA transient, IOP Conference Series: Materials Science and Engineering 123 (2016).
[39] S. Guilbert-Banti, P. Lacote, G. Taraud, P. Berger, J. Desquines, C. Duriez, Influence of hydrogen on the oxygen solubility in Zircaloy-4, Journal of Nuclear Materials 469 (2016) 228-236.
[40] A. Sawatzky, A proposed criterion for the oxygen embrittlement of Zircaloy-4 fuel cladding, Zirconium in the Nuclear Industry (Fourth Conference), ASTM STP 681, American Society for Testing and Materials, 1979, pp. 479-496.
[41] H.M. Chung, A.M. Garde, T.F. Kassner, Development of an Oxygen Embrittlement Criterion for Zircaloy Cladding Applicable to Loss-of-Coolant Accident Conditions in Light-Water Reactors, Zirconium in the Nuclear Industry (Fourth Conference), ASTM STP 681, American Society for Testing and Materials, 1979, pp. 600-627.
[42] P. Bossis, B. Verhaeghe, S. Doriot, D. Gilbon, V. Chabretou, A. Dalmais, J.P. Mardon, M. Blat, A. Miquet, In PWR comprehensive study of high burn-up corrosion and growth behavior of M5® and recrystallized low-tin Zircaloy-4, Journal of ASTM International 6 (2009) 1-27.
[43] M. Große, E. Lehmann, M. Steinbrück, G. Kühne, J. Stuckert, Influence of oxide layer morphology on hydrogen concentration in tin and niobium containing zirconium alloys after high temperature steam oxidation, Journal of Nuclear Materials 385 (2009) 339-345.
[44] M. Große, M. Steinbrueck, B. Shillinger, A. Kaestner, In-situ Investigations of the Hydrogen Uptake of Zirconium Alloys during Steam Oxidation, Zirconium in the Nuclear Industry: 18th International Symposium, ASTM STP 1597, R. Comstock and A. Motta, Eds., ASTM International, West Conshohocken, PA, 2018, 1114-1135.
[45] D. Gosset, M. Le Saux, In-situ X-ray diffraction analysis of zirconia layer formed on zirconium alloys oxidized at high temperature, Journal of Nuclear Materials 458 (2015) 245-252.

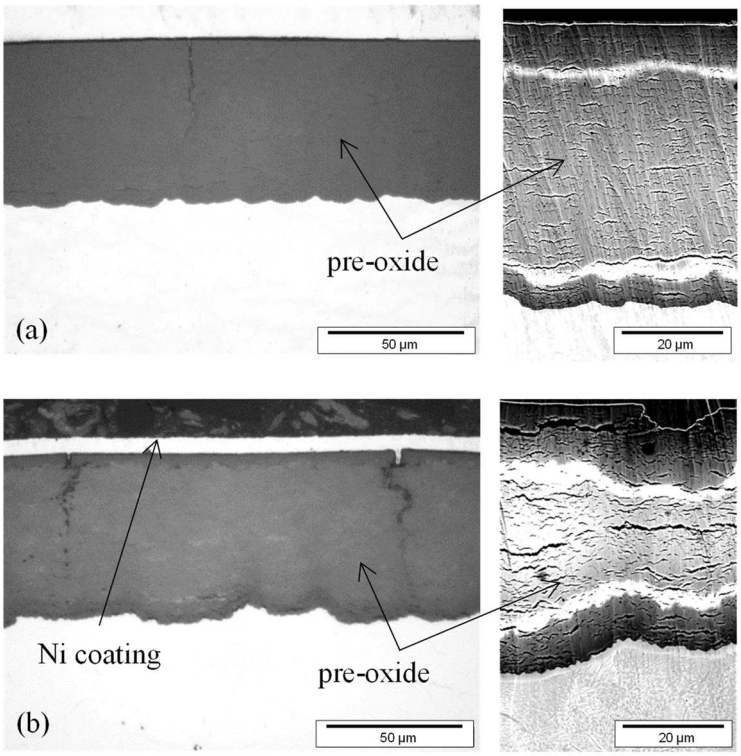

Fig. 1. Optical micrographs (left) and field emission gun scanning electron microscopy micrographs (right) of transverse cross-sections of Zy-4 samples with pre-oxide layers (a) of 59 µm-thick formed under static water at 360°C and (b) 50 µm-thick formed in air at 550°C.

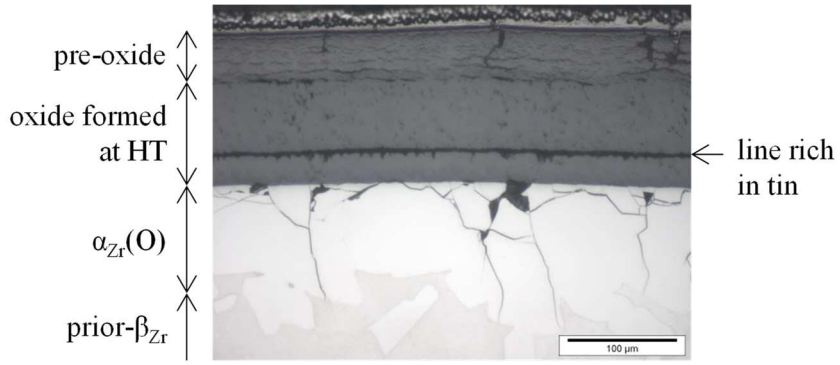

Fig. 2. Optical micrograph of a transverse cross-section of a Zy-4 sample with 59 µm-thick pre-oxide layers formed under static water at 360°C oxidized during 600s under steam at 1200°C.

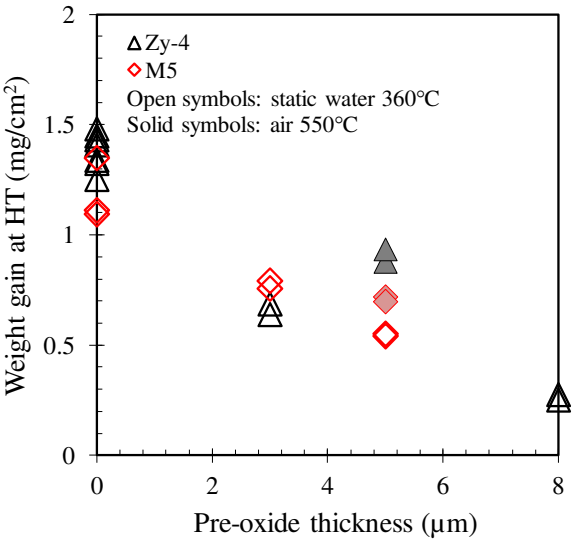

Fig. 3. Evolution of the weight gain of Zy-4 and $M5_{Framatome}$ after steam oxidation during 600s at 850°C, as a function of the pre-existing oxide layer thickness formed under either static water at 360°C or air at 550°C.

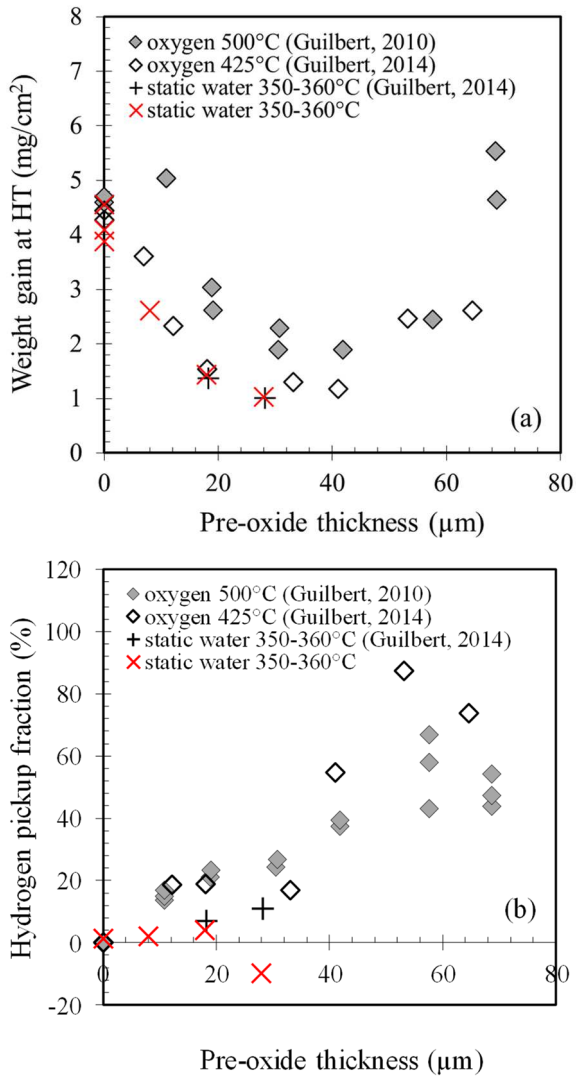

Fig. 4. Evolution of (a) the weight gain and (b) the hydrogen pickup fraction of Zy-4 steam oxidized during 6000s at 900°C, as a function of the pre-existing oxide layer thickness formed under either static water at 350-360°C; comparison to the results obtained by Guilbert *et al.* [10][11] on Zy-4 samples pre-oxidized under either O_2 at 500°C or 425°C or static water at 350-360°C.

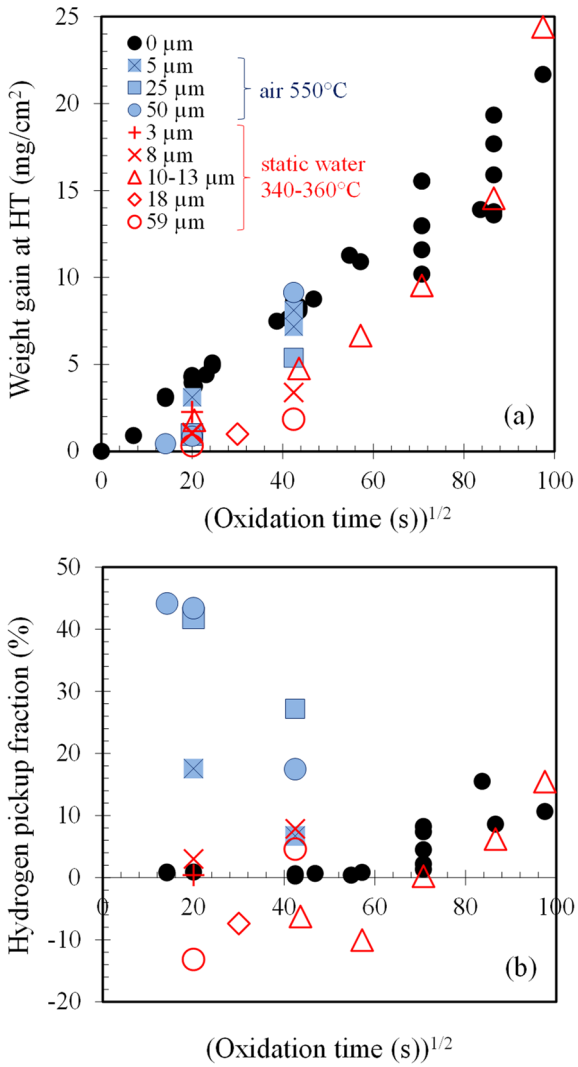

Fig. 5. Evolution of (a) the weight gain and (b) the hydrogen pickup fraction as a function of the oxidation time under steam at 1000°C for Zy-4, as-received and with various pre-oxide thicknesses formed under either air at 550°C or static water at 340-360°C.

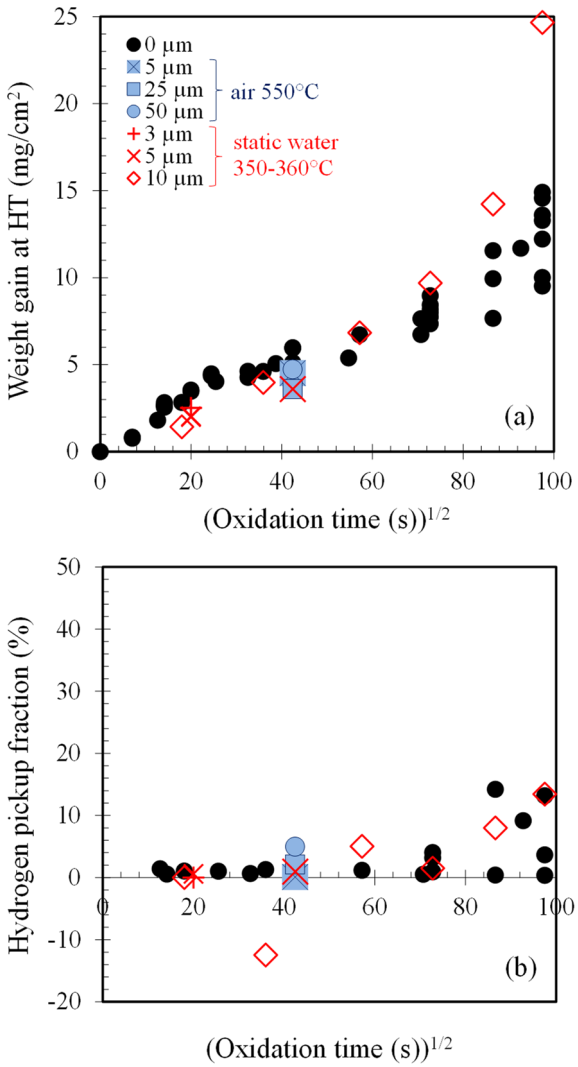

Fig. 6. Evolution of (a) the weight gain and (b) the hydrogen pickup fraction as a function of the oxidation time under steam at 1000°C for $M5_{Framatome}$, as-received and with various pre-oxide thicknesses formed under either air at 550°C or static water at 340-360°C.

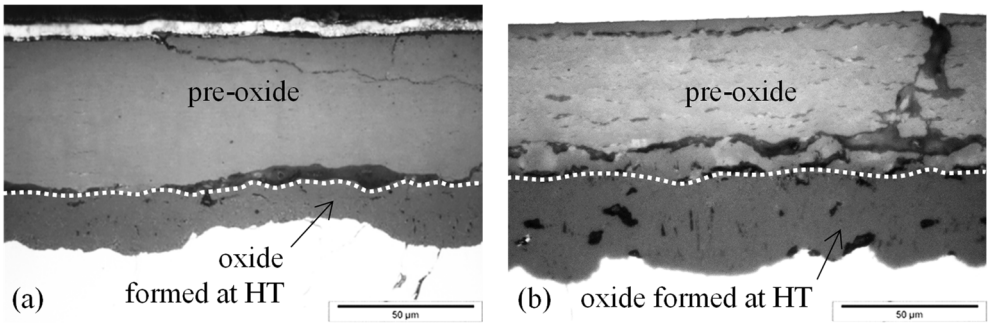

Fig. 7. Optical micrographs of transverse cross-sections of Zy-4 samples with pre-oxide layers (a) of 59 µm-thick formed under static water at 360°C and (b) 50 µm-thick formed in air at 550°C, steam oxidized during 1800s at 1000°C.

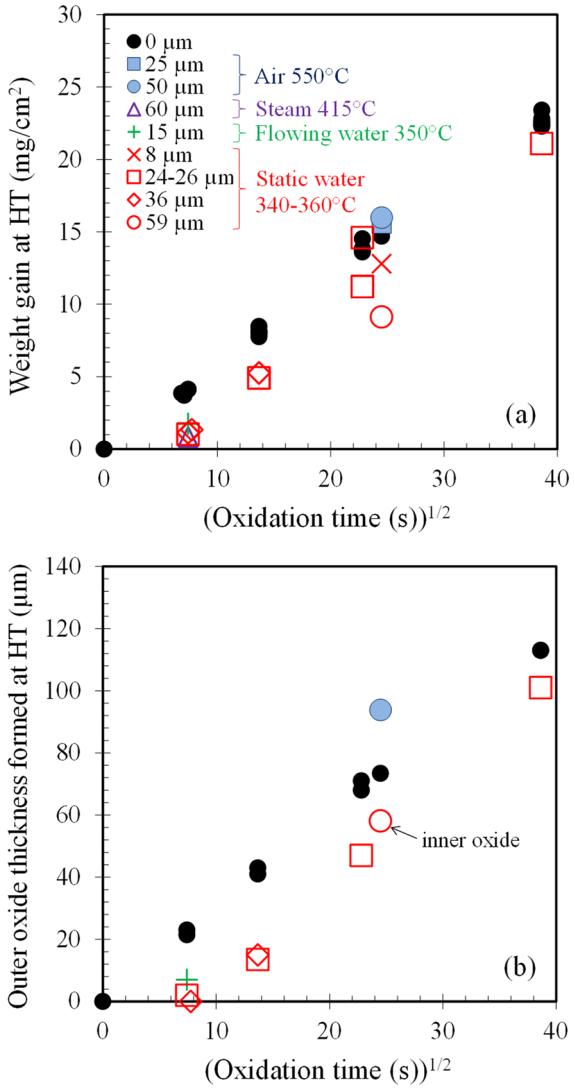

Fig. 8. Evolution of (a) the weight gain and (b) the thickness of the outer oxide layer formed during steam oxidation at 1200°C, as a function of the oxidation time for Zy-4, as-received and with various pre-oxide thicknesses formed under either air at 550°C, steam at 415°C, flowing water at 350°C or static water at 340-360°C.

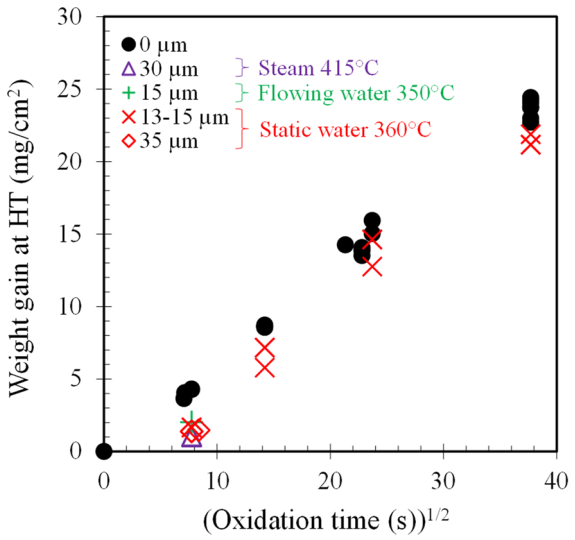

Fig. 9. Evolution of the weight gain as a function of the oxidation time under steam at 1200°C, for $M5_{Framatome}$, as-received and with various pre-oxide thicknesses formed under either steam at 415°C, flowing water at 350°C or static water at 360°C.

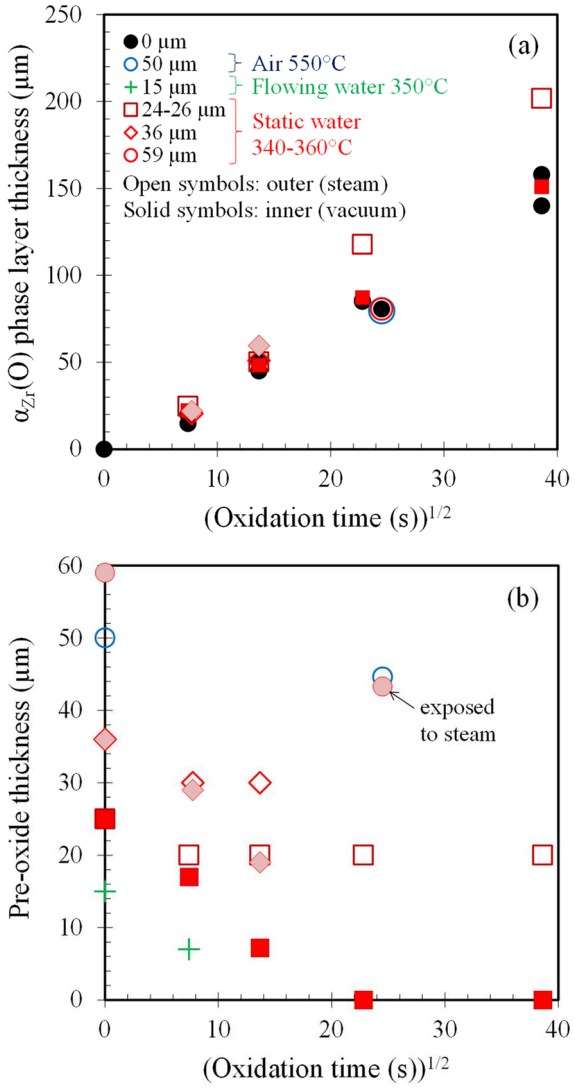

Fig. 10. Evolution of the thickness of (a) the "continuous" α_{Zr}(O) phase layers and (b) the remaining pre-oxide layers at the outer and inner peripheries respectively exposed to steam and vacuum (unless otherwise stated), as a function of the oxidation time at 1200°C for Zy-4, as-received and with various pre-oxide thicknesses formed under either flowing water at 350°C, static water at 340-360°C or air at 550°C.

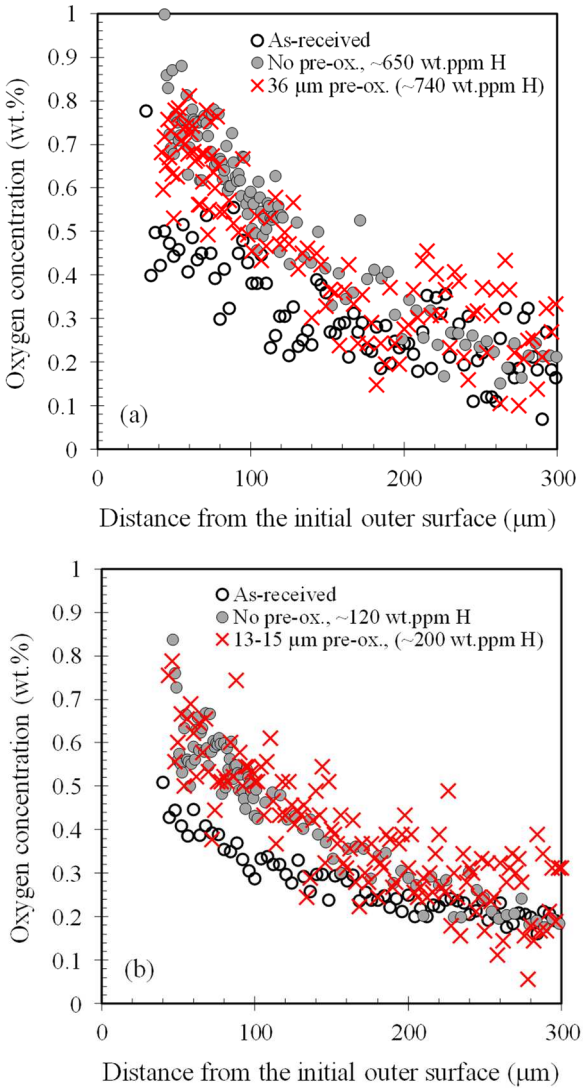

Fig. 11. Oxygen concentration profiles (EPMA) across the half thickness (from the initial outer surface of the cladding sample) for (a) Zy-4 and (b) M5, non-pre-oxidized (as-received and pre-hydrided) and pre-oxidized under static water at 360°C, steam oxidized during 55-60s at 1200°C.

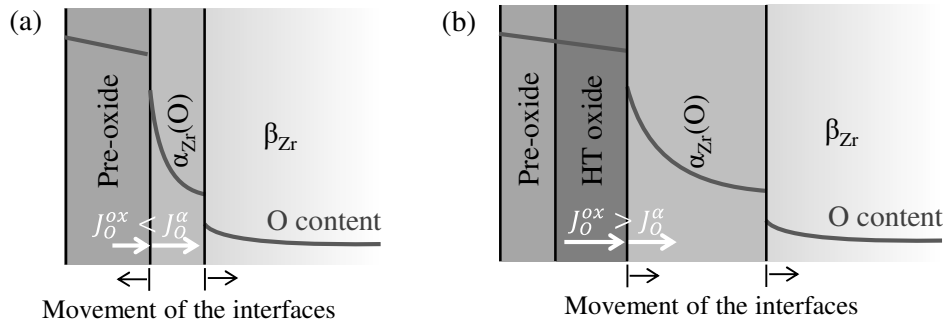

Fig. 12. Schematic representation of the oxidation process of pre-oxidized materials under steam at HT: (a) reduction of the pre-oxide at the beginning of the holding at HT, then (b) growth of a new oxide at HT at the metal oxide interface.

Table 1

Data available in the literature relative to the effect of a pre-oxide layer on the steam HT oxidation of Zy-4 and $M5_{Framatome}$ (n/a: not available).

Mate-rial	Outer / inner pre-ox. thick-ness (µm)	Pre-oxidation conditions	HT steam oxidation conditions	Weight gain and oxide thickness compared to the non-pre-oxidized material	Hydrogen pick-up at HT	Ref.
Zy-4	60 / 60	Water 340°C to 20 µm of pre-ox. then O_2 400°C	1008-1240°C, 300-2400s	Lower at the beginning of oxidation, then close	n/a	[1]
	50 / 50	n/a	1100°C, 120-3600s	Lower for ox. times ≤ 1800s at 1100°C, then close	n/a	[2]
	few-50 / few-50	Steam 350-600°C	1000-1200°C, 300s	Lower for pre-ox. < 10 µm, close or higher for thicker pre-oxides	n/a	[3]
	few-50 / few-50	Steam 400-800°C	1000-1200°C, 300s	Lower at 1000 and 1100°C but not at 1200°C	n/a	[4]
	5-10 / 5-10	n/a 817°C	982-1316°C, 6-558s	Lower, the thicker the pre-ox. the larger the difference	n/a	[5] [6]
	~1 / ~1	Water 300°C	900-1100°C, 60-5000s	Slightly lower at 900 and 950°C, similar at 1000 and 1100°C	n/a	[7]
	4-7 / 4-7	Water + steam 650°C	700-850°C, 60-1500s	Lower, the thicker the pre-ox. and the lower the temperature the larger the difference	n/a	[8]
	6 / 6	Steam 450°C 103 bar	900-1200°C, 2400s	Lower, the lower the temperature the larger the difference	n/a	[9]
	30 and 80 / 30 and 80	Air 500°C (after gaseous hydriding 400°C)	900-1200°C, 2400s	Lower, the lower the temperature the larger the difference, higher for 80 µm-thick than for 30 µm-thick pre-ox.	n/a	[9]
	10-70 / 10-70	O_2 500°C	900°C, 6000s	Lower, increasing difference with increasing pre-ox. thickness below 40 µm, decreasing beyond	Significant for pre-ox. < 40 µm-thick, large for thicker pre-ox.	[10]
	7-64 / 7-64	O_2 425°C	900-1200°C, 100-6000s	Lower, increasing difference with increasing pre-ox. thickness below 40 µm, decreasing beyond at 900 and 1000°C	Significant for 7-12 µm-thick pre-ox., low for 18-32 µm-thick, large for pre-ox. > 40 µm	[11]
	18 and 28 / 18 and 28	Water 350-360°C	900°C, 6000s 1000°C, 900s	Lower	Not significant	[11]
	20 and 50 / 20 and 50	Steam 500°C	700-900°C, 1500s	Lower, no significant difference between 20 and 50 µm-thick pre-ox.	n/a	[12]
	8 / 8	Steam 500°C	800°C, 1500s	Lower	n/a	[13]
	50-85 / 50-85	Flowing water 350°C	1000-1300°C, n/a	Close	n/a	[14]
	71-95 / 11±4	PWR	1200°C, 62-206s	Lower	n/a	[15]
	68 / 11±4	PWR	1200°C, 174-534s	Slightly lower	Slightly negative	[15]
	40-44 / 11±4	PWR	1200°C, 174-323s	Slightly lower	Significant	[15]
	~30 / n/a	PWR	1204°C, 300-1200s	Close	n/a	[17]
	~30? / n/a	PWR	1000-1200°C, 120-2760s	Slightly lower at the beginning of ox. at 1000 and 1100°C, close at 1200°C	n/a	[18]
	7-56 / n/a	PWR	1030-1200°C, 300-2400s	Lower, the thicker the pre-ox. and the lower the temperature the larger the difference	n/a	[1]

	Up to 80-100 / n/a	PWR	1050-1300°C, n/a	Close	n/a	[14]
M5	12±1 / 8±3	PWR	1200°C, 220-360s	n/a	Not significant	[15]
	6-7 / few	PWR	1000-1200°C, 120-2760s	Close at the inner surface, lower at 1000°C, slightly lower at 1100°C and close at 1200°C at the outer surface	n/a	[19]

Table 2

Nominal chemical compositions (in wt%) of the studied materials.

Material	Sn	Fe	Cr	Nb	O	Zr
Zircaloy-4	1.3	0.2	0.1	-	0.13	balance
$M5_{Framatome}$	-	0.04	-	1.0	0.14	balance

Table 3

Conditions of pre-oxidation, pre-oxide thicknesses and hydrogen contents after pre-oxidation, and conditions of oxidation under steam at HT, for Zy-4.

Conditions of pre-oxidation	outer / inner pre-oxide thickness (µm)	Hydrogen content (wppm.)	HT steam oxidation conditions	Facility used for HT oxidation, oxidation type (1S: one-side oxidation; 2S: two-side oxidation)
No pre-oxidation	-	-	600s at 850°C	CINOG HP, 2S
			6000s at 900°C	DEZIROX 1, 2S
			50, 420, 534, 1700, 1900, 2193,3270, 5000, 7000, 7500 and 9500s at 1000°C	DEZIROX 1, 1S
			200, 400, 1500, 1800, 3000, 5000, 7500 and 9500s at 1000°C	DEZIROX 1, 2S
			200, 400, 600 and 1800s at 1000°C	CINOG HP, 2S
			55, 187, 520 and 1492s at 1200°C	DEZIROX 1, 1S
			600s at 1200°C	DEZIROX 1, 2S
Air 550°C	5 / 5	22	600s at 850°C	CINOG HP, 2S
			400 and 1800s at 1000°C	DEZIROX 1, 2S
Air 550°C	25 / 25	84	400 and 1800s at 1000°C	DEZIROX 1, 2S
			600s at 1200°C	DEZIROX 1, 2S
Air 550°C	50 / 50	182	200, 400 and 1800s at 1000°C	DEZIROX 1, 2S
			600s at 1200°C	DEZIROX 1, 2S
Steam 415°C	~60 / 60	3339	55s at 1200°C	DEZIROX 1, 1S
Static water 360°C (autoclave)	3 / 3	69*	600s at 850°C	CINOG HP, 2S
			400s at 1000°C	CINOG HP, 2S
Static water 360°C (autoclave)	8 / 8	123	6000s at 900°C	DEZIROX 1, 2S
			600s at 850°C	CINOG HP, 2S
			400s at 1000°C	CINOG HP, 2S
			1800s at 1000°C	DEZIROX 1, 2S
Static water 340°C (autoclave)	~10-13 / 10-13	~200-383	420, 1900, 3270, 5000, 7500 and 9500s at 1000°C	DEZIROX 1, 1S
Static water 350°C (autoclave)	~18 / 18	367	6000s at 900°C	DEZIROX 1, 2S
			900s at 1000°C	DEZIROX 1, 2S
Static water 360°C (autoclave)	~24-26 / 24-26	~500-600	55, 187, 520, 1492s at 1200°C	DEZIROX 1, 1S
Static water 360°C (autoclave)	~28 / 28	~726	6000s at 900°C	DEZIROX 1, 2S
			900s at 1000°C	DEZIROX 1, 2S
Static water 360°C (autoclave)	~36 / 36	~734-739*	55-60 and 187s at 1200°C	DEZIROX 1, 1S
Static water 360°C (autoclave)	~59 / 59	~997-1008	400 and 1800s at 1000°C	DEZIROX 1, 2S
			600s at 1200°C	DEZIROX 1, 2S
Flowing water 350°C (Reggae loop)	~15 / 5	~150-200*	55s at 1200°C	DEZIROX 1, 1S

* content estimated from measurements on equivalent samples or from available correlations between weight gain and hydrogen content

Table 4

Conditions of pre-oxidation, pre-oxide thicknesses and hydrogen contents after pre-oxidation, and conditions of oxidation under steam at HT, for $M5_{Framatome}$.

Conditions of pre-oxidation	outer / inner pre-oxide thickness (µm)	Hydrogen content (wppm.)	HT steam oxidation conditions	Facility used for HT oxidation, oxidation type (1S: one-side oxidation; 2S: two-side oxidation)
No pre-oxidation	-	-	600s at 850°C	CINOG HP, 2S
			200, 400, 600 and 1800s at 1000°C	CINOG HP, 2S
			50, 160, 323, 650, 1060, 1290, 3270, 5292, 7500, 8600 and 9500s at 1000°C	DEZIROX 1, 1S
			1500, 1800, 3000, 5000, 7500 and 9500s at 1000°C	DEZIROX 1, 2S
			50, 202, 455, 520, 562 and 1422s at 1200°C	DEZIROX 1, 1S
Air 550°C	5 / 5	17*	600s at 850°C	CINOG HP, 2S
			1800s at 1000°C	DEZIROX 1, 2S
Air 550°C	25 / 25	26	1800s at 1000°C	DEZIROX 1, 2S
Air 550°C	50 / 50	72	1800s at 1000°C	DEZIROX 1, 2S
Steam 415°C	~30 / 30	1154	60s at 1200°C	DEZIROX 1, 1S
Static water 360°C (autoclave)	3 / 3	25*	600s at 850°C	CINOG HP, 2S
			400s at 1000°C	CINOG HP, 2S
			1800s at 1000°C	DEZIROX 1, 2S
Static water 350°C (autoclave)	~10 / 10	193-210	323, 1290, 3270, 5292, 7500 and 9500s at 1000°C	DEZIROX 1, 1S
Static water 360°C (autoclave)	~13-15 / 13-15	~144-241*	60, 202, 562 and 1422s at 1200°C	DEZIROX 1, 1S
Static water 360°C (autoclave)	~35 / 35	~178-280*	60-70s at 1200°C	DEZIROX 1, 1S
Flowing water 350°C (Reggae loop)	~15 / 5	~150-200*	60s at 1200°C	DEZIROX 1, 1S

* content estimated from measurements on equivalent samples or from available correlations between weight gain and hydrogen content